

Nucleon spin structure studies at Jefferson Lab

A. Deur

Thomas Jefferson National Accelerator Facility

(Dated: May 21, 2019)

We report on the low and moderate Q^2 nucleon spin structure measurements done at Jefferson Lab, examining specifically the inclusive program. We discuss what the data teach us about quark confinement and the emergence of the effective hadronic degrees of freedom from the fundamental partonic ones. We show how this experimental program has reached its goal by providing a precise mapping at low, intermediate and moderately high Q^2 which has followed in many advances, e.g., with Chiral Perturbation Theory. Another example of a recent advance imputable to the JLab spin data is the improved understanding of α_s at low energy, which allowed Light-Front Holographic QCD, an approximation to non-perturbative QCD, to derive the hadron spectrum from Λ_s .

I. INTRODUCTION

There are many reasons to study the spin of the nucleon. An ingenious reason is that it is interesting in itself: we are curious to know how the spin of the nucleon emerges from its constituents, i.e., how the spins and orbital angular momenta of the quarks and gluons combine together into the spin 1/2 of the nucleon. We have also more practical reasons: spin degrees of freedom provide additional tests to theories. Hence, studying spin observables provides a more complete study of the fundamental force ruling the nucleon structure, the Strong Force, of which the accepted gauge theory is Quantum Chromodynamics (QCD). We can also learn about important emergent properties of QCD, such as the mechanism of confinement, how the effective hadronic degrees of freedom stem from the fundamental partonic ones, or how well non-perturbative methods, e.g., Chiral Perturbation Theory (χ Pt), Lattice Gauge Theory or the gravity-gauge (AdS/CFT) correspondence, describe the Strong Force in its low energy domain. Finally, a precise knowledge of polarized parton distributions is necessary for investigations of physics beyond the standard model or high precision atomic physics. We have thus many good reasons to be interested in the nucleon spin.

In this document, we will focus on what spin structure studies teach us about confinement, the emergence of the hadronic degrees of freedom and tests of non-perturbative approaches to QCD. Due to space limits, we will discuss results based on inclusive lepton scattering, which are only a fraction of the polarized observables necessary for a full description of the nucleon spin structure. In fact, we will focus on the first moment of the spin structure function g_1 at low to moderate Q^2 . These results were obtained with the 6 GeV JLab accelerator. The future spin program with the new 12 GeV JLab beam is discussed in V. Burkert's contribution to these proceedings.

II. INCLUSIVE POLARIZED LEPTON SCATTERING

Inclusive polarized lepton scattering data, obtained by experiments in which the only particle of the reaction de-

tected is the scattered lepton, is parametrized (neglecting the weak interaction) by four structure functions: two unpolarized ones: $F_1(x, Q^2)$ and $F_2(x, Q^2)$, and two polarized ones: $g_1(x, Q^2)$ and $g_2(x, Q^2)$ (x is the Bjorken scaling variable and $Q^2 = -q^2$, with $q \equiv (\nu, \vec{q})$ the 4-momentum exchanged between the beam particle and the target particle). In the Bjorken limit, $Q^2 \rightarrow \infty$ while Q^2/ν stays finite, $F_1(x)$ and $F_2(x)$ are constructed from the quark densities $u(x)(\bar{u}(x))$, $d(x)(\bar{d}(x))$, $s(x)(\bar{s}(x))...$ which provide the amount of up, down, strange... quarks (antiquarks) carrying a nucleon momentum fraction x , respectively. $F_1(x)$ and $F_2(x)$ are simple sums of these densities: $F_1 = q_u^2[u + \bar{u}] + q_d^2[d + \bar{d}] + \dots$ and $F_2 = 2xF_1$, with q_f the electric charge of the quark of flavor f . Likewise, $g_1(x)$ is constructed from the quark polarizations $\Delta u(x)...$ which are, for a given x , the difference between the amount of quarks with their spins parallel to the nucleon spin and those with their spins antiparallel: $g_1 = q_u^2[\Delta u + \Delta \bar{u}] + q_d^2[\Delta d + \Delta \bar{d}] + \dots$ In the Bjorken limit the other spin structure function has no role: $g_2 = 0$.

This relatively simple picture is only valid at $Q^2 \rightarrow \infty$ where the QCD coupling α_s should vanish, i.e. in the asymptotic case where quarks are free. At finite (but still large) Q^2 , quarks start to interact, which leads to gluon corrections. Furthermore, the mass of the target M and effects of transverse momentum P_\perp or transverse spin are less suppressed: $M^2/Q^2 \neq 0$, $P_\perp^2/Q^2 \neq 0$ and thus, they start to play a role. This breaks down the above relations: $F_2 \neq 2xF_1$ and $g_2 \neq 0$.

At smaller Q^2 , ($\simeq \text{GeV}^2$), α_s becomes large and the significantly stronger quark interaction induces correlations, known as Higher Twists (HT) effects, which invalidate the simple description summarized above: $F_1 \neq q_u^2[u + \bar{u}] + q_d^2[d + \bar{d}] + \dots$ and $g_1 \neq q_u^2[\Delta u + \Delta \bar{u}] + q_d^2[\Delta d + \Delta \bar{d}] + \dots$. Some of the HT effects that contribute to inclusive polarized scattering have been interpreted recently as the transverse confining force acting on the quarks [1]. HT have been measured in a number of Jefferson Lab (JLab) experiments in Halls A [2], B [3] and C [4]. In particular, the HT were extracted in the high- x domain in [5]. The SANE experiment in Hall C will further add to these data (see W. Armstrong's contribution to these proceedings).

An example of HT extraction specially relevant to this

document is the determination of the twist-4 element f_2^{p-n} [3]. It is extracted from Bjorken sum measurements (see next section) at JLab. Its absolute value at $Q^2 = 1 \text{ GeV}^2$, $f_2^{p-n} = -0.064(35)$, is large (the scale is set by the leading twist value of the Bjorken sum, $\Gamma_1^{p-n,LT} = 0.137(13)$). Such large HT agrees with the intuition that non-perturbative effects should be large at moderate Q^2 . However, the $1/Q^4$ HT correction μ_6 is small and μ_8 is of similar magnitude as f_2 but of opposite sign. Thus, overall the sum of HT is small near $Q^2 = 1 \text{ GeV}^2$. This explains why HT have been so elusive, as well as the onset of hadron-parton duality [6]. If HT are overall small at these Q^2 , what are their actual effects and what is their practical connection to confinement? To answer these questions, we first need to discuss the subject of “sum rules”.

III. SUM RULES

A Sum Rule is a rule (i.e an equality) that relates a sum (i.e., an integral such as a moment of a structure function) to a quantity characterizing the studied particle. A relevant sum rule to this document is the Gerasimov-Drell-Hearn (GDH) sum rule [7] that relates the photo-absorption cross-sections $\sigma^{3/2}$ and $\sigma^{1/2}$ ($3/2$ ($1/2$) indicates that the photon helicity is aligned (anti-aligned) with the target polarization) to the anomalous magnetic moment κ_t of the target:

$$\int_{\nu_{thr}}^{\infty} (\sigma^{3/2}(\nu) - \sigma^{1/2}(\nu)) \frac{d\nu}{\nu} = \frac{2\alpha\pi^2\kappa_t^2}{M^2}, \quad (1)$$

with ν the photon energy, ν_{thr} the photo-production threshold, α the QED coupling constant and M the target mass. Originally derived for photo-production ($Q^2 = 0$), the GDH sum rule has been latter generalized to $Q^2 > 0$ [8]:

$$\Gamma_1 \equiv \int_0^1 g_1(x, Q^2) dx = \frac{Q^2}{8} S_1, \quad (2)$$

where S_1 is a double DVCS spin-dependent amplitude. The famous Bjorken sum rule for spin-dependent deep inelastic scattering (DIS) [9] then appears as the isovector part of the generalized GDH sum rule in the large Q^2 limit:

$$\int_0^1 (g_1^p - g_1^n) dx = \frac{1}{6} \left(1 - \frac{\alpha_s}{\pi} - 3.58 \left(\frac{\alpha_s}{\pi} \right)^2 \dots \right) + \sum_{i=2} \frac{\mu_{2i}}{Q^{2i}}, \quad (3)$$

where the series coefficients and α_s are expressed in the \overline{MS} renormalization scheme (RS), and where the μ_{2i} are non-perturbative HT corrections –discussed in the preceding section– that become important only at low Q^2 . Data on Γ_1^p , Γ_1^n and Γ_1^{p-n} , including preliminary results from experiments EG1, EG4 and E97110 are shown in Fig. 1. The high precision of the mapping at intermediate and moderately-high Q^2 done for the proton and

the neutron at JLab can be seen on Fig. 1 (top plots). The $\Gamma_1(Q^2)$ moments display a strong Q^2 -variation while transiting from high-to-low Q^2 . The mapping is being finalized with the analysis of more recent experiments covering the χPT domain at very low Q^2 (preliminary results shown on the bottom plots). Again, the data have high precision and should test well the χPT predictions. The preliminary results on low- Q^2 measurement of the generalized GDH sum rule on the neutron (^3He) are discussed in C. Peng’s contribution to these proceedings. We see that the recent χPT results agree with the preliminary data. We can also notice the similar negative slopes for Γ_1^p and Γ_1^n at very low Q^2 . This is explained by the similar absolute values of the anomalous magnetic moments of the proton and neutron (assuming the GDH sum rule is not violated, or at least not strongly). Consequently, these slopes mostly cancel in the Bjorken sum Γ_1^{p-n} , which results for this observable in a restoration of the approximate conformal behavior (no Q^2 -dependence) of QCD already seen at large Q^2 . This observation is important in the context of using the AdS/CFT (Anti-de Sitter/Conformal Field Theory) approach to non-perturbative QCD, as we will discuss latter.

Other spin-dependent sum rules exist, such as the Burkhardt-Cottingham sum rule on g_2 [10] or polarizabilities sum rules that involve higher moments of g_1 and g_2 , see C. Peng, J. Zhang and K. Slifer contributions to these proceedings.

The high Q^2 data have historically provided a check of QCD in its spin sector, as well as the measurement of the quark spin contribution to the nucleon spin and –via evolution equations– a first assessment of the gluon spin contribution ΔG (see e.g. [5]). The moderate Q^2 data provide –as discussed in the previous section– a handle on HT. The new low- Q^2 data test recent χPT calculations [11], see C. Peng and K. Slifer contributions to these proceedings. We will discuss now what we learn in practice from these measurements.

IV. INSIGHTS IN THE NON-PERTURBATIVE NUCLEON STRUCTURE

Exploring the connection between hadronic and partonic degrees of freedom was the main goal of the JLab experiments that covered the moderate Q^2 -values that bridge the hadronic and partonic domains. That is, their goal was to provide data to help developing/improving non-perturbative theoretical frameworks, and to help explain how these various theoretical frameworks are connected. We will show here how this goal was achieved.

The precise mapping of low and moderate Q^2 regions motivated:

1. improvement at low Q^2 on χPT calculations [11], in particular to address the δ_{LT} puzzle, see C. Peng, J. Zhang and K. Slifer contributions to these proceedings;

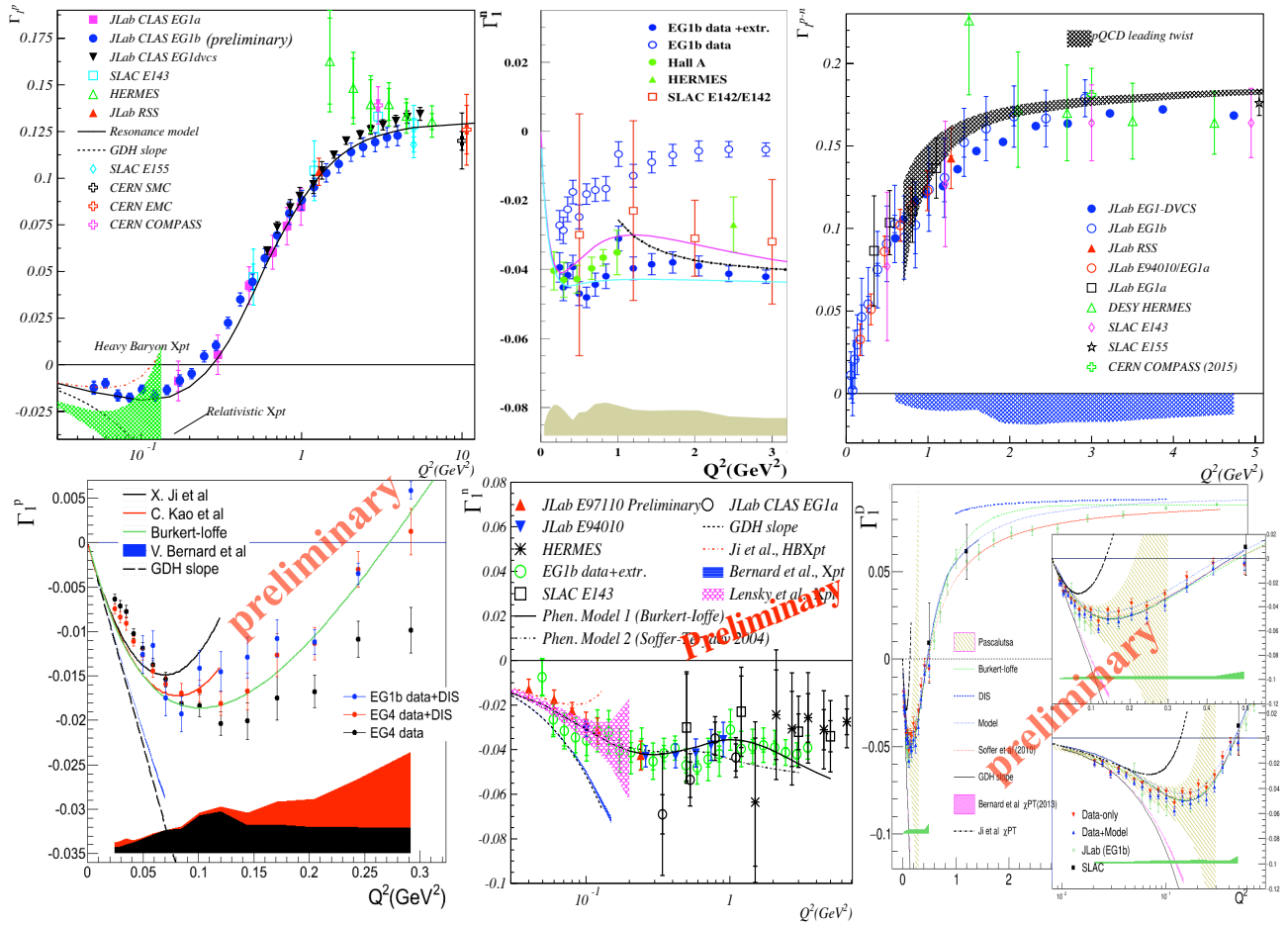


FIG. 1: Top panels: Measurements of Γ_1^p (left), Γ_1^n from D (center) and Γ_1^{p-n} (right). Bottom panels: preliminary low Q^2 results from JLab’s experiments EG4 (p: left; n from D: right) and E97110 (center, n from ^3He).

2. improvement at higher Q^2 of pQCD techniques, such as the Analytic or Massive Perturbation Theories [12]. These approaches essentially fold partially the HT contributions into the definition of α_s [13] in order to extend the domain of applicability of pQCD series to lower Q^2 ;
3. the calculation of α_s using an AdS/CFT duality approach [14].

This is this last item that we will discuss to illustrate how the JLab spin data have pushed fundamental advances in our understanding of non-perturbative QCD.

V. THE LIGHT-FRONT HOLOGRAPHIC QCD APPROXIMATION

The Light-Front Holographic QCD (LFHQCD) approximation to QCD [15] is based on light-front quantization, which allows a rigorous and exact formulation of non-perturbative QCD [16]. In particular, light-front quantization yields a relativistic Schrödinger-like equation describing hadrons as quark bound-states. In prin-

ciple, all elements of this equation can be determined from the QCD Lagrangian; but, in practice, it is only in (1+1) dimensions that we know how to compute the effective confining potential entering the equation [17]. Due to the overwhelming complexity, in (3+1) dimensions, the potential must be determined from other means than first-principle light-front calculations. One such method is the correspondence between gravity in anti-de Sitter (AdS) space and QCD on the light-front [18]. This correspondence originates from the fact that the group of isometries of a 5-dimensional AdS space is the conformal invariance of the dual field theory in Minkowski space, and thus encodes the scale invariance of the classical QCD Lagrangian. The calculations are tractable if short-distance quantum fluctuations are neglected and if the quark masses are set to zero (chiral limit). The 5-dimensional AdS calculations are projected on the 4-dimensional boundary of the AdS space which is identified with the physical Minkowski spacetime (hence the “holographic” denomination). Thus, Light-Front Holography provides a semiclassical approximation to QCD in its long distance regime which incorporates fundamental aspects of QCD.

Enforcing the conformal symmetry of QCD, i.e that the Lagrangian has no energy scale in the chiral limit, without explicitly breaking the symmetry, leads to a unique choice of potential [19]. It has the form of a harmonic oscillator on the light front. The uniqueness of this form is confirmed by the facts that 1) only this form yields a zero-mass pion in the chiral limit [20]; 2) it explains the remarkable mass symmetry between mesons and baryons [21]; 3) it is equivalent to the well-established linear potential for static quarks in the usual instant-form front [22].

Hence, fundamental aspects of nonperturbative QCD are incorporated in LFHQCD which is based on the embedding of light-front relativistic bound state equations in AdS space. This semiclassical approximation to QCD in its large distance domain is completely determined by the constraints imposed by superconformal algebra, a symmetry which can originate from the dynamics of color SU(3) [23]. The only free parameter is the scale κ . In fact, chiral QCD is independent of conventional units of mass such as MeV. In other words, a theory or model of the Strong Force can only predict dimensionless ratios such as the proton to ρ -meson mass ratio M_p/M_ρ , or M_p/Λ_s . For LFHQCD this single parameter is denoted κ . For standard QCD, it is Λ_s . The relation between the two is known analytically and numerically [24] and was obtained *via* the QCD coupling α_s , which we discuss next.

VI. THE QCD COUPLING α_s

A quantity of central interest for this article that can be determined by LFHQCD is the strong coupling α_s [13]. A particularly useful way to define it in the long distance regime is *via* the concept of effective charge [25], which is defined from the perturbative series of an observable, truncated to first order in α_s . For example, with such coupling, Eq. (3) becomes:

$$\int_0^1 (g_1^p - g_1^n) dx \equiv \frac{1}{6} \left(1 - \frac{\alpha_{g_1}}{\pi}\right), \quad (4)$$

where the subscript g_1 reminds us of this particular choice of definition. This choice can be viewed as equivalent to a RS choice [26]. One sees that with this definition, both the short distance pQCD effects (the higher order terms in the leading twists pQCD series) and long distance confinement effects (the HT terms) are now folded into the definition of α_s . This is in analogy with the original coupling constant becoming a running (effective) coupling when short distance quantum effects are folded into its definition [13]. The folding of the long distance confinement effects into the coupling definition regularizes it, removing the unphysical Landau pole at $Q^2 = \Lambda_s^2$ [13]. We already mentioned how the folding of HT lead to optimized perturbative series. The definition of α_s as an effective charge can be viewed as a generalization of this

procedure: the role of HT –or more generally the long distance confining effects– is to regularize α_s .

The Bjorken sum measurement can be used to obtain α_{g_1} [27]. The most important data are from JLab at moderate and low Q^2 . At lower and higher Q^2 , the GDH and Bjorken sum rules, respectively, can supplement the data. The experimental data yield the coupling shown in Fig. 2. An important observation provided by the mea-

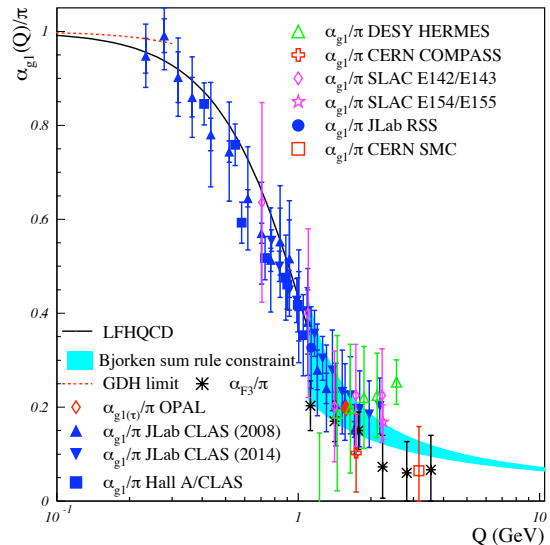


FIG. 2: The effective charge α_{g_1}/π from experimental data (symbols). The data are supplemented at low Q^2 by the GDH sum rule (dashed line) and at high Q^2 by the Bjorken sum rule (band). The LFHQCD prediction is given by the continuous line.

surement of α_{g_1} at low Q^2 is that it freezes, i.e., QCD’s approximate conformal behavior is restored. (QCD is also conformal at large Q^2 , a phenomenon called Bjorken Scaling). This allows us to apply LFHQCD at low Q^2 . It predicts that [14]:

$$\alpha_s(Q^2) = \pi e^{-\frac{Q^2}{4\kappa^2}}. \quad (5)$$

This prediction agrees well with the data, see Fig. 2. It is important to remember that there are no free parameters in Eq. (5), κ being determined by hadron masses (in Fig. 2, $\kappa = M_\rho/\sqrt{2}$ [15]). The LFHQCD prediction is drawn in Fig. 2 up to $Q^2 \simeq 1 \text{ GeV}^2$, its expected domain of validity. At higher Q^2 , short distance quantum effects, which are not included in the usual semiclassical approximation in LFHQCD become important and void the prediction. There, however, pQCD is available to calculate α_{g_1} . In fact, the respective domains of applicability of LFHQCD and pQCD appear to overlap around $Q^2 \simeq 1 \text{ GeV}^2$ [26]. This allows us to match the α_{g_1} computation from pQCD to that from LFHQCD, thereby relating hadronic masses to the fundamental QCD parameter Λ_s [24]. For example, the leading order relation

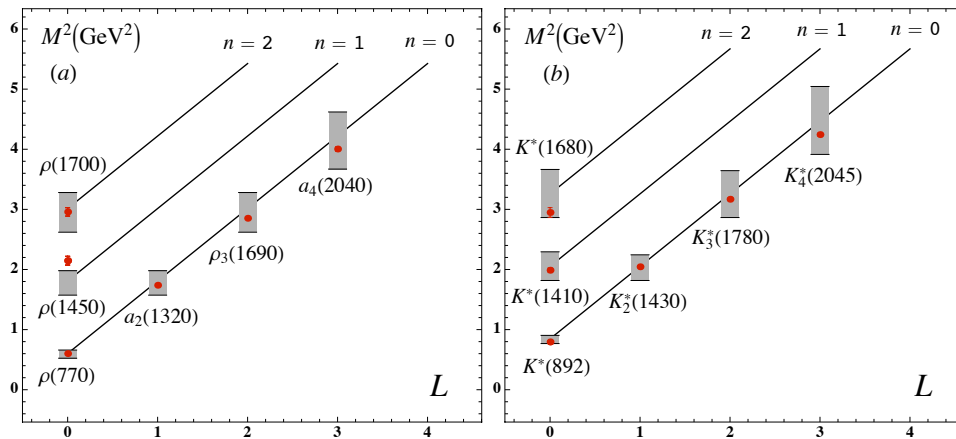


FIG. 3: The predicted mass spectrum from LFHQCD for unflavored (a) and strange light vector mesons (b). The gray bands represent the uncertainty. The points are the experimental values.

between $\Lambda_{\overline{MS}}$ and M_ρ is:

$$\Lambda_{\overline{MS}} = M_\rho e^{-a}/\sqrt{a}, \quad (6)$$

where $a = 4(\sqrt{\ln(2)^2 + 1 + \beta_0/4} - \ln(2))/\beta_0$, ($\beta_0 = 11 - 2n_f/3$ is the first coefficient of the QCD's β -series). Numerically, $a \simeq 0.55$ for $n_f = 3$ quark flavors. At N³LO the numerical relation is $\Lambda_{\overline{MS}} = 0.440M_\rho$. The ρ meson is the ground state solution of the LFHQCD Schrödinger equation, i.e., with radial excitation $n = 0$ and internal orbital angular momentum $L = 0$. Higher mass states are solutions with $n \neq 0$ and $L \neq 0$ and are shown on Fig. 3, together with a similar prediction for strange mesons. Baryon masses can be obtained similarly or thanks to the mass symmetry between mesons and baryons [21]. Conversely, the known value of κ can be used with the same matching procedure to predict Λ_s . This leads to $\Lambda_{\overline{MS}}^{n_f=3} = 0.339(19)$ GeV, which agrees well with the world average value of $0.339(17)$ GeV [28].

VII. SUMMARY AND CONCLUSION

We have reported on the low and moderate Q^2 (few GeV²) nucleon spin structure measurements done at JLab, focusing on the inclusive program on the experimental side. On the phenomenology side, we focused on what this teaches us about quark confinement and the emergence of effective degrees of freedom (hadrons) from the fundamental ones (quark and gluons). The JLab data cover an extensive kinematic range with high precision thanks to the high luminosity of the experimental equipment. They complement the data from the CERN, SLAC and DESY high energy facilities. Most of the data at moderate Q^2 are now available. Remaining data from the CLAS EG1b and Hall C SANE experiments will be available soon. The analysis of the lower Q^2 data is being finalized for the neutron, both from polarized deuteron and ³He targets, and should be available early

2017. More work remains for the low Q^2 proton data. Finally, some very low Q^2 data ($\approx 0.01 < Q^2 < 0.04$ GeV²) from n (³He) should become available in the upcoming years.

We argued that the JLab spin sum rule program has reached its goal: it has provided a precise mapping at low, intermediate and moderately high Q^2 and triggered advances on the theoretical front. In particular, there is good progress in the description of the Strong Force over the full Q^2 -range, with improvements in the Chiral Perturbation Theory calculations (low Q^2) and pQCD series (high Q^2). A goal for these data was to help understanding how hadronic degrees of freedom connect to partonic ones. Better measurements and understanding of Higher Twists, as well as new approaches to the confinement problem, e.g., from Light-Front Holographic QCD, represent advances on this front. As examples of recent developments directly connected to the JLab spin data, we showed the extraction of the QCD coupling α_s and its determination from Light-Front Holographic QCD, whose applicability domain overlaps with that of pQCD near $Q \simeq 1$ GeV. This overlap allows the analytical determination of the hadron spectrum with Λ_s as the only input. One parameter e.g., Λ_s allows one to express quantities in terms of conventional GeV units. Since Λ_s is well determined, the mass spectrum prediction from Light-Front Holographic QCD has no free parameters. Obtaining such result has been the long-thought goal of the Strong Force studies. Arguably Light-front holographic QCD is not QCD, but it is a semiclassical approximation which incorporates basics aspects of nonperturbative QCD dynamics which are not apparent from the QCD Lagrangian, such as the emergence of a mass scale and confinement, the existence of a zero mass particle in the chiral limit and universal Regge trajectories [23]. Hence the derivation of the strong coupling in the infrared domain and the hadron spectrum represents an important advance toward reaching this long-thought goal, and the Jefferson Lab spin data has played a major role in it.

Acknowledgments

We thank S. J. Brodsky, E. Chudakov, V. Sulkosky, G. F. de T eramond and N. Ton for their useful comments

on the manuscript. This material is based upon work supported by the U.S. Department of Energy, Office of Science, Office of Nuclear Physics under contract DE-AC05-06OR23177.

-
- [1] M. Burkardt, Phys. Rev. D **88**, 114502 (2013)
- [2] X. Zheng *et al.*, Phys. Rev. C **70**, 065207 (2004); K. Kramer *et al.*, Phys. Rev. Lett, **95**, 142002 (2005); Z.-E. Meziani *et al.*, Phys. Lett. B **613**, 148 (2005); M. Posik *et al.*, Phys. Rev. Lett, **13**, 022002 (2014)
- [3] A. Deur *et al.*, Phys. Rev. Lett. **93**, 212001 (2004); Phys. Rev. D **78**, 032001 (2008); Phys. Rev. D **90**, no. 1, 012009 (2014); A. Deur, nucl-ex/0508022; Y. Prok *et al.*, *et al.*, Phys. Lett. B **672**, 12 (2009); Phys. Rev. C **90**, 025212 (2014)
- [4] K. Slifer *et al.*, Phys. Rev. Lett, **105**, 101601 (2010)
- [5] E. Leader *et al.*, Phys. Rev. D **75**, 074027 (2007)
- [6] E. D. Bloom and F. J. Gilman, Phys. Rev. Lett. **25**, 1140 (1970)
- [7] S. B. Gerasimov, Sov. J. Nucl. Phys. **2**, 430 (1966) [Yad. Fiz. **2**, 598 (1965)]; S. D. Drell and A. C. Hearn, Phys. Rev. Lett. **16**, 908 (1966)
- [8] X. D. Ji and J. Osborne, J. Phys. G **27**, 127 (2001)
- [9] J. D. Bjorken, Phys. Rev. **148**, 1467 (1966); Phys. Rev. D **1**, 1376 (1970)
- [10] H. Burkhardt and W. N. Cottingham, Annals Phys. **56**, 453 (1970)
- [11] V. Bernard *et al.*, Phys. Rev. D **87** 054032 (2013); V. Lensky, J. M. Alarcon and V. Pascalutsa, Phys. Rev. C **90** 055202 (2014)
- [12] R. S. Pasechnik, J. Soffer and O. V. Teryaev, Phys. Rev. D **82** 076007 (2010); A. A. Natale, Nucl. Phys. Proc. Suppl. **199** 178 (2010); D. V. Shirkov, Phys. Part. Nucl. Lett. **10** 186 (2013)
- [13] A. Deur, S. J. Brodsky and G. F. de T eramond, Prog. Part. Nucl. Phys. **90**, 1 (2016)
- [14] S. J. Brodsky, G. F. de T eramond and A. Deur, Phys. Rev. D **81**, 096010 (2010)
- [15] S. J. Brodsky, G. F. de T eramond, H. G. Dosch and J. Erlich, Phys. Rep. **05** 001 (2015)
- [16] S. J. Brodsky, H. C. Pauli and S. S. Pinsky, Phys. Rept. **301**, 299 (1998)
- [17] K. Hornbostel, S. J. Brodsky and H. C. Pauli, Phys. Rev. D **41**, 3814 (1990)
- [18] S. J. Brodsky and G. F. de T eramond, Phys. Rev. Lett. **96**, 201601 (2006), Phys. Rev. Lett. **102**, 081601 (2009)
- [19] S. J. Brodsky, G. F. de T eramond and H. G. Dosch, Phys. Lett. B **729**, 3 (2014)
- [20] H. G. Dosch, G. F. de T eramond and S. J. Brodsky, Phys. Rev. D **91**, no. 8, 085016 (2015)
- [21] G. F. de T eramond, H. G. Dosch and S. J. Brodsky, Phys. Rev. D **91**, no. 4, 045040 (2015)
- [22] A. P. Trawinski, S. D. Glazek, S. J. Brodsky, G. F. de T eramond and H. G. Dosch, Phys. Rev. D **90**, no. 7, 074017 (2014)
- [23] G. F. de T eramond, S. J. Brodsky, A. Deur, H. G. Dosch and R. S. Sufian, arXiv:1611.03763 [hep-ph]
- [24] A. Deur, S. J. Brodsky and G. F. de T eramond, Phys. Lett. B **750**, 528 (2015); A. Deur, S. J. Brodsky and G. F. de T eramond, arXiv:1608.04933 [hep-ph]
- [25] G. Grunberg, Phys. Lett. B **95** 70 (1980); Phys. Rev. D **29** 2315 (1984); *ibid* **40** 680(1989).
- [26] A. Deur, S. J. Brodsky and G. F. de T eramond, Phys. Lett. B **757**, 275 (2016)
- [27] A. Deur, V. Burkert, J. P. Chen and W. Korsch, Phys. Lett. B **650**, 244 (2007); Phys. Lett. B **665**, 349 (2008)
- [28] C. Patrignani *et al.* [Particle Data Group Collaboration], Chin. Phys. C **40**, no. 10, 100001 (2016)